Prebuckling and Buckling analysis of Variable Angle Tow Plates with general boundary conditions

Gangadharan Raju[a], Zhangming Wu[a], Byung Chul Kim[a], Paul Weaver[a,*]

[a] *Advanced Composite Centre for Innovation and Science, Department of Aerospace Engineering, Queens Building, University Walk.*

Abstract

The concept of Variable angle tow placement is explored for enhancing the buckling resistance of composite plates subjected to axial compression under different plate boundary conditions. The buckling problem of VAT plate is complicated because of variation in stiffness properties across planform of the plate due to curvilinear fiber path distribution. The problem requires prebuckling analysis to be performed first to determine the non-uniform stress distribution and then the buckling analysis of VAT plates. In the present work, a solution methodology based on the Differential quadrature method (DQM) is developed for solving the partial differential equations of VAT plates with linear fiber angle orientations. Within the framework of DQM, a stress function formulation for inplane analysis and displacement formulation for buckling analysis was employed to derive the governing differential equations based on classical laminated plate theory. The novel aspect of the present work is the use of Airy's stress function to model the prebuckling analysis of VAT plates which considerably reduces the problem size and computational effort. This approach provides more generality to handle pure stress and mixed boundary conditions more effectively when compared to the exisiting analytical models. Furthermore, the governing differential equation derived for buckling analysis of VAT panels considers the effect of bending-twist coupling terms on the buckling load. DQM was applied first to solve the inplane elasticity problem of VAT plates subjected to cosine distributed compressive loads. DQM was then extended to solve the inplane problem of VAT plates under uniform end shortening for which the unknown stress distribu-

*Corresponding author

Email address: paul.weaver@bristol.ac.uk (Paul Weaver)

tions are non-uniform. Stress distributions along the edges of the plate were expanded using Legendre polynomials and the unknown coefficients were determined using a least square approach such that the displacment boundary conditions are satisfied. Later, the DQM was applied to solve the buckling problem of rectangular VAT plates subjected to axial compression under different boundary conditions, *viz*., simply supported, clamped and free edge boundary conditions. Comparisons were made with finite element results obtained using ABAQUS and the accuracy and efficiency of the proposed DQM approach were studied.

Keywords: Buckling, Variable Angle Tow composites, Airy's stress function, Differential Quadrature Method

---

1. Introduction

The use of laminated composites for design of aerospace structures allows the stiffness, strength and flexibility to be controlled in different directions. In conventional laminates, the fiber angles are kept constant in a lamina which results in constant stiffness properties across the planform of the plate and limited tailorability options. Two commonly used approaches reported in literature to improve the structural response by allowing in-plane tailorability of composites are 1) adding patches of additional layers with different fiber orientations 2) varying the fiber orientation angles over the planform of the plate. Biggers *et. al.* (1; 2) employed piecewise uniform redistribution of layers with specified orientations to create beneficial stiffness distributions across the planform of the plate. This resulted in better buckling performance of composite plates and used finite element models to compute the crtical buckling load. Hyer *et. al* (3; 4) initiated the use of curvilinear fiber paths aligned along the principal directions of the stress fields for impoving the buckling resistance of composite plate with a hole. They used finite elements to model the buckling problem and then determined optimal fiber distribution in each element to achieve better buckling peformance. Nagendra *et. al* (5) used non-uniform rational B-splines for designing fiber variation in the planform of the plate and performed FE analysis to optimise the fiber design based on buckling load and natural frequency. Gurdal *et. al* (6) varied the stiffness properties by introducing linear fiber variation definition along the length of the composite laminate and employed an iterative collocation numerical technique to solve the inplane response of a VAT panel governed by a system

of coupled equilibrium equations expressed in terms of displacements. Senocak *et. al* (7) used galerkin method and polynomial trial functions to solve the inplane response of composite plate with varying fiber content and linearily varying fiber orientations. The existing models for inplane analysis of VAT plates is based on displacement formulation which requires an iterative strategy to acheive the desired accuracy. This approach is computationally expensive due to the number of iterations involved and also application of pure stress or mixed boundary conditions becomes quite difficult. Gurdal *et. al* (8) studied the buckling response of variable stiffness panels by allowing the stiffness variation along the loading direction and perpendicular to the loading direction. They employed Rayleigh-Ritz (RR) method to compute the buckling coefficient which did not include the effect of flexural-twist coefficients D_{16}, D_{26}. Alhajahmad*et. al* (9) used variable stiffness concept to study the pressure pillowing problem of fuselage skin. They used Rayleigh-Ritz method to perform nonlinear analysis and designed plates with optimal fiber paths for maximum failure load. Weaver*et. al* (10) designed and manufactured variable stiffness panels using an embroidery based process. Their FE results showed similar buckling performance of VAT panels when compared to quasi-isoropic laminate, but exhibited superior post-buckling behavior. Most of the work reported in literature for analysis of VAT panels use finite element (FE) method and require more elements for accurate solutions. Furthermore, when FE method is coupled with optimisation algorithms, the analysis becomes computationally expensive. To overcome this drawback, new methods are required which are fast, accurate, general and easily integrable with optimisation algorithms for design of VAT panels. As an alternative approach to variational methods, the Differential Quadrature Method (DQM) is investigated in this work for structural analysis of VAT panels. DQM is an efficient and straight forward discretization technique for obtaining accurate numerical solution with less computational effort.

DQM introduced by Bellman *et. al.* (11) is based on the assumption that the partial derivatives of function in one direction can be expressed as a linear combination of functional values at all the grid points along that direction. DQM require fewer grid points to compute solutions with reasonable accuracy when compared to FE analysis. DQM has been successfully applied to solve various problems in structural mechanics (13) and the results demonstrate the potential as an attractive numerical technique. The key issue in the application of DQM is to determine the weighting coefficients and non-uniform grid distribution for approximating the partial derivatives

of the function. Shu *et. al* (12) developed a generalised DQM approach for handling various structural problems more effectively and demonstrated the accuracy of the method. Darvizeh *et. al.* (15) compared the performance of DQM with RR method for buckling analysis of composite plates and the study showed the accuracy and reliability of DQM. Wang*et. al.* (16) studied the buckling of thin plates subjected to nonlinearly distributed edge compression loads using DQM. Sherbourne *et. al.* (14) studied the effect of grid distribution in buckling analysis of anisotropic composite plates and reported that using non uniform grids gives better results compared to uniform grids.

In this paper, numerical methodology based on the DQM is developed for buckling analysis of VAT panels. The new aspect of the present work is the use of Airy's stress function to perform the prebuckling analysis of anisotropic VAT plates which considerably reduces the problem size and when coupled with DQM requires less computational effort. The generality of the formulation helps in efficient modelling of pure stress and mixed inplane boundary conditions applied to the VAT plate. Also, the governing differential equations for buckling analysis of VAT composite plate includes the effect of flexural-twist coupling coefficients. The buckling performance of VAT panels with linear fiber orientations under different boundary conditions was then studied using DQM and the results were validated using finite element (FE) method. The stability and robustness of DQM in computing the buckling performance of VAT panels were studied.

The remainder of this paper is organized as follows. In the next section, the numerical aspects of DQM such as choice of test functions, grid point distributions and approaches to apply boundary conditions are discussed. The concept of variable stiffness is introduced in section 3 and the prebuckling analysis formulation of VAT panels using DQM are presented in section 4. The DQM fomulation for buckling analysis of VAT panels under different boundary conditons are discussed in section 5. In section 6, several numerical examples of VAT panels are presented to demonstrate the accuracy of the method and close with a few concluding remarks in section 7.

2. Differential Quadrature Method

The method of differential quadrature is a numerical discretization technique for approximating the partial derivatives of a function with respect to a spatial variable, using a weighted linear combination of function values at some intermediate points in that variable. For example, the n^{th} order partial

derivative of a function *f(x)* at the i^{th} discrete point is approximated by

$$\frac{\partial^n f(x_i)}{\partial x^n} = A_{ij}^{(n)} f(x_j) \quad i = 1, 2, ..., N, \tag{1}$$

where x_i= set of discrete points in the x direction; and $A_{ij}^{(n)}$ is the weighting coefficients of the n^{th} derivative and repeated index j means summation from 1 to N. The weighting coefficients and the grid distribution determine the accuracy of the DQM results. For determining the weighting coefficients, the function *f(x)* must be approximated using test functions. Lagrange interpolation polynomial and Fourier series expansion are the commonly used test functions in DQM. In this work, Lagrange interpolation polynomial are chosen as test functions for the computation of weighting coefficients and are given by

$$g_k(x) = \frac{M(x)}{(x - x_k)M^{(1)}(x_k)} \quad k = 1, 2, ..N \tag{2}$$

where

$$M(x) = \prod_{j=1}^{N}(x - x_j), \quad M^{(1)}(x_i) = \frac{\partial M(x_i)}{\partial x} = \prod_{j=1, j\neq i}^{N}(x_i - x_j) \tag{3}$$

The weighting coefficient for the first order derivative are explicitly defined by

$$A_{ij}^{(1)} = \frac{M^{(1)}(x_i)}{(x_i - x_j)M^{(1)}(x_j)}, \quad i \neq j, \quad i, j = 1, 2..N \quad A_{ii}^{(1)} = -\sum_{j=1, i\neq j}^{N} A_{ij}^{(1)} \tag{4}$$

where x_i are the coordinates of the grid points. The second and higher order weighting coefficients can be obtained from $A_{ij}^{(1)}$ using matrix multiplication and is explained in detail by Shu (12). In this work, the non uniform grid distribution given by the Chebyshev-Gauss-Labotto points are used for the computation of weighting matrices and is given by

$$X_i = \frac{1}{2}[1 - cos(\frac{i-1}{N-1}\pi)], \quad i = 1, 2, ...N \tag{5}$$

where N is the number of grid points.

Different methods have been reported in literature for proper implementation of boundary conditions using the DQM. In this work, the direct substitution method proposed by Shu *et. al.* (17; 18) has been used to implement

the different plate boundary conditions. Using the above approach, the essential boundary conditions are implemented along the boundary points and the force boundary conditions are discretized using DQM and applied to grid points adjacent to the boundary points. In this work, the governing differential equations for buckling analysis of symmetric VAT panel are derived and DQM was applied to solve the buckling problem under different boundary conditions.

3. Variable angle tow panels

The concept of VAT placement provides the designer a wider design space for tailoring the composite structure for enhanced structural performance under prescribed loading conditions. Numerous benefits are achieved using VAT placement, for example, by blending (minimising) stiffness variations between structural components (e.g. stiffener to skin) to reduce inter-laminar stresses. Also, the in-plane fiber orientation and local thickness distribution can be tailored to reduce the need for discrete stiffening and opening up the possibility of lightweight, stiffener-free skins.

In this work, VAT panels with fiber orientation angle variation along one direction and constant stiffness properties in the other direction is considered for analysis. A VAT plate with linear fiber angle variation is considered for analysis (6) and the angle variation along the x direction is given by

$$\theta(x) = \phi + \frac{2(T_1 - T_0)}{a}|x| + T_0 \tag{6}$$

where T_0 is the fiber orientation angle at the panel center $x = 0$, T_1 is the fiber orientation angle at the panel ends $x = \pm a/2$ and ϕ is the angle of rotation of the fiber path.

In VAT panels, stiffness (A, B, D matrices) vary with $x-y$ coordinates resulting in non-uniform in-plane stress distribution under constant edge loads or displacements (8) and evaluation of these distributions is critical for buckling load solutions. Gurdal *et. al* (8) derived a set of coupled elliptic partial differential equations based on the displacement formulation for prebuckling analysis of VAT plates. They used a numerical tool (ELLPACK) directly to solve the coupled equilibrium equations on displacement fields based on an iterative strategy to achieve solution of desired accuracy. The stress function formulation when applied to model the prebuckling problem of VAT plates

results in a fourth order partial differential equation. This formulation reduces the number of differential equations to be solved by DQM and requires less computational effort. The stress function formulation allows more efficient modelling of pure stress and mixed boundary conditions for prebuckling analysis which is explained in detail in the next section.

4. Prebuckling analysis

For symmetric VAT composite plates, the midplane strains(ϵ^0) in terms of stress resultants($\bar{N}$) can be expressed using the following relation given by,

$$\begin{Bmatrix} \epsilon_x^0 \\ \epsilon_y^0 \\ \epsilon_{xy}^0 \end{Bmatrix} = \begin{bmatrix} A_{11}^*(x,y) & A_{12}^*(x,y) & A_{16}^*(x,y) \\ A_{12}^*(x,y) & A_{22}^*(x,y) & A_{26}^*(x,y) \\ A_{16}^*(x,y) & A_{26}^*(x,y) & A_{66}^*(x,y) \end{bmatrix} \begin{Bmatrix} \bar{N}_x \\ \bar{N}_y \\ \bar{N}_{xy} \end{Bmatrix} \tag{7}$$

where $A^*(x,y)$ is the inplane compliance matrix. The Airy's stress functions and the strain compatability condition was used to solve the in-plane response of symmetric VAT panels. A stress function Ω is introduced such that

$$\bar{N}_x = \Omega_{,yy}, \quad \bar{N}_y = \Omega_{,xx}, \quad \bar{N}_{xy} = -\Omega_{,xy} \tag{8}$$

The compatability condition in terms of mid-plane strains in a plane stress condition is given by

$$\epsilon_{x,yy}^0 + \epsilon_{y,xx}^0 - \epsilon_{xy,xy}^0 = 0 \tag{9}$$

Making use of Eq. 8 in conjuction with Eq. 9, the condition of compatability is expressed as,

$$\begin{aligned} &(A_{11}^*(x,y)\Omega_{,yy} + A_{12}^*(x,y)\Omega_{,xx} - A_{16}^*(x,y)\Omega_{,xy})_{,yy} + \\ &(A_{12}^*(x,y)\Omega_{,yy} + A_{22}^*(x,y)\Omega_{,xx} - A_{26}^*(x,y)\Omega_{,xy})_{,xx} + \\ &(-A_{16}^*(x,y)\Omega_{,yy} - A_{26}^*(x,y)\Omega_{,xx} + A_{66}^*(x,y)\Omega_{,xy})_{,xy} = 0 \end{aligned} \tag{10}$$

Differentiation and reordering gives

$$\begin{aligned} &A_{11}^*(x,y)\Omega_{,yyyy} - 2A_{16}^*(x,y)\Omega_{,xyyy} + (2A_{12}^*(x,y) + A_{66}^*(x,y))\Omega_{,xxyy} \\ &-2A_{26}^*(x,y)\Omega_{,yyyy} + A_{22}^*(x,y)\Omega_{,xxxx} + (2A_{11y}^*(x,y) - A_{16,x}^*(x,y))\Omega_{,yyy} \\ &+(2A_{12,x}^*(x,y) - 3A_{16,y}^*(x,y) + A_{66,x}^*(x,y))\Omega_{,xyy} + (2A_{12,y}^*(x,y) - 3A_{26,x}^*(x,y) + \\ &A_{66,y}^*(x,y))\Omega_{,xxy} + (2A_{22,x}^*(x,y) - A_{26,y}^*(x,y))\Omega_{,xxx} + \\ &(A_{11,yy}^*(x,y) + A_{12,xx}^*(x,y) - A_{16,xy}^*(x,y))\Omega_{,yy} + (-A_{26,xx}^*(x,y) - A_{16,yy}^*(x,y) + \\ &A_{66,xy}^*(x,y))\Omega_{,xy} + (A_{12,yy}^*(x,y) + A_{22,xx}^*(x,y) - A_{26,xy}^*(x,y))\Omega_{,xx} = 0 \end{aligned} \tag{11}$$

Thus, the Eq. 11 represents a fourth order elliptic partial differential equation in terms of stress function with variable coefficients. The number of differential terms with variable coefficients in Eq. 11 indicates more degree of freedom available for tailoring VAT plates when compared to straight fiber composites. The DQM representation of the Eq. 11 is given by,

$$
\begin{aligned}
&A^*_{11}(x,y)\sum_{m=1}^{N_y} B^{(4)}_{jm}\Omega_{im} - 2A^*_{16}(x,y)\sum_{k=1}^{N_x}\sum_{m=1}^{N_y} A^{(1)}_{ik}B^{(3)}_{jm}\Omega_{km} \\
&+(2A^*_{12}(x,y)+A^*_{66}(x,y))\sum_{k=1}^{N_x}\sum_{m=1}^{N_y} A^{(2)}_{ik}B^{(2)}_{jm}\Omega_{km} - 2A^*_{26}(x,y)\sum_{k=1}^{N_x}\sum_{m=1}^{N_y} A^{(3)}_{ik}B^{(1)}_{jm}\Omega_{km} \\
&+A^*_{22}(x,y)\sum_{k=1}^{N_x} A^{(4)}_{ik}\Omega_{kj} + (2A^*_{11y}(x,y) - A^*_{16,x}(x,y))\sum_{m=1}^{N_y} B^{(3)}_{jm}\Omega_{im} \\
&+(2A^*_{12,x}(x,y) - 3A^*_{16,y}(x,y) + A^*_{66,x}(x,y))\sum_{k=1}^{N_x}\sum_{m=1}^{N_y} A^{(1)}_{ik}B^{(2)}_{jm}\Omega_{km} \\
&+(2A^*_{12,y}(x,y) - 3A^*_{26,x}(x,y) + A^*_{66,y}(x,y))\sum_{k=1}^{N_x}\sum_{m=1}^{N_y} A^{(2)}_{ik}B^{(1)}_{jm}\Omega_{km} \\
&+(2A^*_{22,x}(x,y) - A^*_{26,y}(x,y))\sum_{k=1}^{N_x} A^{(3)}_{ik}\Omega_{kj} \\
&+(A^*_{11,yy}(x,y) + A^*_{12,xx}(x,y) - A^*_{16,xy}(x,y))\sum_{m=1}^{N_y} B^{(2)}_{jm}\Omega_{im} \\
&+(-A^*_{26,xx}(x,y) - A^*_{16,yy}(x,y) + A^*_{66,xy}(x,y))\sum_{k=1}^{N_x}\sum_{m=1}^{N_y} A^{(1)}_{ik}B^{(1)}_{jm}\Omega_{km} \\
&+(A^*_{12,yy}(x,y) + A^*_{22,xx}(x,y) - A^*_{26,xy}(x,y))\sum_{k=1}^{N_x} A^{(3)}_{ik}\Omega_{kj} = 0 \\
&i = 1,...,N_x; \quad j = 1,N_y
\end{aligned}
\tag{12}
$$

where N_x, N_y are the number of grid points in the x and y directions respectively. The stress boundary conditions expressed in terms of Ω and its derivatives were applied along the boundary grid points. For non-uniform axial compression loading, the boundary conditions are given by,

$$
\begin{aligned}
&\frac{\partial^2\Omega}{\partial y^2}|_{x=0,a} = \sigma_x(y), \quad \frac{\partial^2\Omega}{\partial x^2}|_{y=0,b} = 0, \quad \frac{\partial^2\Omega}{\partial x\partial y}|_{x=0,a;y=0,b} = 0, \\
&\Omega|_{x=0,y=b} = \frac{\partial\Omega}{\partial x}|_{x=0,y=b} = \frac{\partial\Omega}{\partial y}|_{x=0,y=b} = 0.
\end{aligned}
\tag{13}
$$

The above boundary conditions were expressed in DQM form and assembled with Eq.12, which results in a set of algebraic linear equations. Thus, the

DQM representation for in-plane analysis of symmetric VAT plates in matrix form can be written as,

$$\begin{bmatrix} K_{bb} & K_{bd} \\ K_{db} & K_{dd} \end{bmatrix} \begin{Bmatrix} \Omega_b \\ \Omega_d \end{Bmatrix} = \begin{Bmatrix} F_b \\ 0 \end{Bmatrix} \tag{14}$$

where F_b is the generalised force vector. The subscripts b denote the boundary and their adjacent grid points for applying the boundary conditions. The subscript d refers to the domain grid points. The Eq. 14 is solved for Ω and the stress resultant distributions can be computed using the following DQM equations,

$$\begin{aligned} \bar{N}_x &= \sum_{m=1}^{N_y} B_{jm}^{(2)} \Omega_{im} \\ \bar{N}_y &= \sum_{k=1}^{N_x} A_{ik}^{(2)} \Omega_{kj} \\ \bar{N}_{xy} &= -\sum_{k=1}^{N_x} \sum_{m=1}^{N_y} A_{ik}^{(1)} B_{jm}^{(1)} \Omega_{km} \\ i &= 1, ..., N_x; \quad j = 1, N_y \end{aligned} \tag{15}$$

The above approach can also be extended to solve the inplane response of VAT plate under uniform axial compression. The axial stress distributions along the edges of the VAT panel corresponding to uniform axial compression is non-uniform and has to be determined. In order to satisfy the uniform displacement boundary conditions, the non-uniform stress distribution $\sigma_x(y)$ along the edge was assumed to be of the form,

$$\sigma_x(y) = \sum_{k=1}^{n} C_k P_k, \tag{16}$$

where C_n are the unknown cofficients and P_n are the Legendre polynomials. In this work Legendre polynomials are chosen for analysis due to superior

convergence properties and defined as,

$$P_1 = 1,\ P_2 = \xi,\ P_3 = \frac{1}{2}(3\xi^2 - 1)\ \cdots$$
$$P_{i+1}(\xi) = \sum_{j=0}^{J}(-1)^j \frac{(2i-2j)!}{2^i j!(i-j)!(i-2j)!}\xi^{i-2j} \tag{17}$$
$$J = \frac{i}{2}(i = 0, 2, 4, \cdots),\ \ \frac{i-1}{2}(i = 1, 3, 5, \cdots)$$

The $\sigma_x(y)$ load distribution corresponding to each Legendre polynomial was applied along the edge of the VAT plate and the corresponding axial displacment distribution u_n is evaluated using the expression,

$$u_n = \int_0^a \left(A^*_{11}(x,y)\phi_{,yy} + A^*_{12}(x,y)\phi_{,xx} - A^*_{16}(x,y)\phi_{,xy}\right) dx. \tag{18}$$

The unknown coefficients C_n were computed by using least squares method to fit u_n with the given displcament boundary condition along the edge $u|_{x=0,a}$. The $\sigma_x(y)$ distribution corresponding to uniform displacment loading was evaluated using Eq. 16. and are given as input for buckling analysis.

5. Buckling analysis

The moment equilibrium equation for symmetrical VAT plate is given by,

$$\frac{\partial^2 M_x}{\partial x^2} + 2\frac{\partial^2 M_{xy}}{\partial x \partial y} + \frac{\partial^2 M_y}{\partial y^2} + \bar{N}_x\frac{\partial^2 w}{\partial x^2} + 2\bar{N}_{xy}\frac{\partial^2 w}{\partial x \partial y} + \bar{N}_y\frac{\partial^2 w}{\partial y^2} + q = 0 \tag{19}$$

where M_x, M_y, M_{xy} are the moment distributions and q is the load applied in z direction. The moment distributions are related to the midplane curvatures by the following relation,

$$\begin{Bmatrix} M_x \\ M_y \\ M_{xy} \end{Bmatrix} = \begin{bmatrix} D_{11}(x,y) & D_{12}(x,y) & D_{16}(x,y) \\ D_{12}(x,y) & D_{22}(x,y) & D_{26}(x,y) \\ D_{16}(x,y) & D_{26}(x,y) & D_{66}(x,y) \end{bmatrix} \begin{Bmatrix} \kappa^0_x \\ \kappa^0_y \\ \kappa^0_{xy} \end{Bmatrix} \tag{20}$$

where D is the laminate bending stiffness matrix and the curvatures are given by $\kappa^0_x = \frac{\partial^2 w}{\partial x^2}, \kappa^0_y = \frac{\partial^2 w}{\partial y^2}, \kappa^0_{xy} = 2\frac{\partial^2 w}{\partial x \partial y}$. Eq. 20 is then substituted in Eq.

19 and the resulting governing differential equation for buckling analysis of symmetrical VAT composite plate is given by

$$\begin{aligned}&D_{11}(x,y)w_{,xxxx}+4D_{16}(x,y)w_{,xxxy}+2(D_{12}(x,y)+2D_{66}(x,y))w_{,xxyy}+\\&4D_{26}(x,y)w_{,yyyx}+D_{22}(x,y)w_{,yyyy}+2(D_{11,x}(x,y)+D_{16,y}(x,y))w_{,xxx}\\&+(6D_{16,x}(x,y)+2D_{12,y}(x,y)+4D_{66,y}(x,y))w_{,xxy}+(2D_{12,x}(x,y)+\\&4D_{66,x}(x,y)+6D_{26,y}(x,y))w_{,xyy}+2(D_{26,x}(x,y)+D_{22,y}(x,y))w_{,yyy}\\&+(D_{11,xx}(x,y)+2D_{16,xy}(x,y)+D_{12,yy}(x,y))w_{,xx}+(2D_{16,xx}(x,y)+\\&4D_{66,xy}(x,y)+2D_{26,yy}(x,y))w_{,xy}+(D_{12,xx}(x,y)+2D_{26,xy}(x,y)+\\&D_{22,yy}(x,y))w_{,yy}+\bar{N}_x w_{,xx}+2\bar{N}_{xy}w_{,xy}+\bar{N}_y w_{,yy}=0\end{aligned} \tag{21}$$

where w is the out-of-plane displacement. The differential terms associated with the derivatives of bending stiffness coefficients have to be considered for accurate buckling load solutions. The DQM representation of Eq. (21) is given by

$$\begin{aligned}&D_{11}(x,y)\sum_{k=1}^{N_x}A_{ik}^{(4)}w_{kj}+4D_{16}(x,y)\sum_{k=1}^{N_x}\sum_{m=1}^{N_y}A_{ik}^{(3)}B_{jm}^{(1)}w_{km}\\&+2(D_{12}(x,y)+2D_{66}(x,y))\sum_{k=1}^{N_x}\sum_{m=1}^{N_y}A_{ik}^{(2)}B_{jm}^{(2)}w_{km}+4D_{26}(x,y)\sum_{k=1}^{N_x}\sum_{m=1}^{N_y}A_{ik}^{(1)}B_{jm}^{(3)}w_{km}\\&+D_{22}(x,y)\sum_{m=1}^{N_y}B_{jm}^{(4)}w_{im}+2(D_{11,x}(x,y)+D_{16,y}(x,y))\sum_{k=1}^{N_x}A_{ik}^{(3)}w_{kj}\\&+(6D_{16,x}(x,y)+2D_{12,y}(x,y)+4D_{66,y}(x,y))\sum_{k=1}^{N_x}\sum_{m=1}^{N_y}A_{ik}^{(2)}B_{jm}^{(1)}w_{km}+(2D_{12,x}(x,y)\\&+4D_{66,x}(x,y)+6D_{26,y}(x,y))\sum_{k=1}^{N_x}\sum_{m=1}^{N_y}A_{ik}^{(1)}B_{jm}^{(2)}w_{km}+2(D_{26,x}(x,y)\\&+D_{22,y}(x,y))\sum_{m=1}^{N_y}B_{jm}^{(3)}w_{im}+(D_{11,xx}(x,y)+2D_{16,xy}(x,y)+D_{12,yy}(x,y))\sum_{k=1}^{N_x}A_{ik}^{(2)}w_{kj}\\&+(2D_{16,xx}(x,y)+4D_{66,xy}(x,y)+2D_{26,yy}(x,y))\sum_{k=1}^{N_x}\sum_{m=1}^{N_y}A_{ik}^{(1)}B_{jm}^{(1)}w_{km}\\&+(D_{12,xx}(x,y)+2D_{26,xy}(x,y)+D_{22,yy}(x,y))\sum_{m=1}^{N_y}B_{jm}^{(2)}w_{im}+\bar{N}_x\sum_{k=1}^{N_x}A_{ik}^{(2)}w_{kj}\\&+2\bar{N}_{xy}\sum_{k=1}^{N_x}\sum_{m=1}^{N_y}A_{ik}^{(1)}B_{jm}^{(1)}w_{km}+\bar{N}_y\sum_{m=1}^{N_y}B_{jm}^{(2)}w_{im}=0\\&\\&i=1,....,N_x;\quad j=1,....,N_y\end{aligned} \tag{22}$$

where $A_{ik}^{(n)}, B_{jm}^{(n)}$ are the n^{th} order partial derivatives with respect to x and y directions respectively. The different plate boundary conditions considered in this work are,
Simply supported edges (SSSS)

$$\begin{aligned} &x = 0, a; \quad w = 0; \quad M_x = -D_{11}(x,y)\frac{\partial^2 w}{\partial x^2} - D_{12}(x,y)\frac{\partial^2 w}{\partial y^2} - 2D_{16}(x,y)\frac{\partial^2 w}{\partial x \partial y} = 0 \\ &y = 0, b; \quad w = 0; \quad M_y = -D_{12}(x,y)\frac{\partial^2 w}{\partial x^2} - D_{22}(x,y)\frac{\partial^2 w}{\partial y^2} - 2D_{26}(x,y)\frac{\partial^2 w}{\partial x \partial y} = 0 \end{aligned} \tag{23}$$

Clamped edges (CCCC)

$$\begin{aligned} &x = 0, a; \quad w = 0; \quad \frac{\partial w}{\partial x} = 0 \\ &y = 0, b; \quad w = 0; \quad \frac{\partial w}{\partial y} = 0 \end{aligned} \tag{24}$$

Simply supported along three edges and one edge free (SSSF)

$$\begin{aligned} &x = 0, a; \quad w = 0; \quad M_x = -D_{11}(x,y)\frac{\partial^2 w}{\partial x^2} - D_{12}(x,y)\frac{\partial^2 w}{\partial y^2} - 2D_{16}(x,y)\frac{\partial^2 w}{\partial x \partial y} = 0 \\ &y = 0; \quad w = 0; \quad M_y = -D_{12}(x,y)\frac{\partial^2 w}{\partial x^2} - D_{22}(x,y)\frac{\partial^2 w}{\partial y^2} - 2D_{26}(x,y)\frac{\partial^2 w}{\partial x \partial y} = 0 \\ &y = b; \quad V_y = -2D_{16}(x,y)\frac{\partial^3 w}{\partial x^3} - D_{22}(x,y)\frac{\partial^3 w}{\partial y^3} - 4D_{26}(x,y)\frac{\partial^3 w}{\partial x \partial^2 y} \\ &\quad - (D12(x,y) + 4D66(x,y))\frac{\partial^3 w}{\partial^2 x \partial y} - (D12_{,y}(x,y) + 2D16_{,x}(x,y)\frac{\partial^2 w}{\partial x^2}) \\ &\quad - (D22_{,y}(x,y) + 2D26_{,x}(x,y)\frac{\partial^2 w}{\partial y^2}) - (2D26_{,y}(x,y) + 4D66_{,x}(x,y)\frac{\partial^2 w}{\partial x \partial y}) = 0 \end{aligned} \tag{25}$$

where V_y is the shear force distribution along the free edge of the plate. The DQM form of simply supported boundary conditions are given by

$$\begin{aligned} &x = 0, a; \quad w_{ij} = 0; \\ &D_{11}(x,y)\sum_{k=1}^{N_x} A_{ik}^{(2)} w_{kj} - D_{12}(x,y)\sum_{m=1}^{N_y} B_{jm}^{(2)} w_{im} - 2D_{16}(x,y)\sum_{k=1}^{N_x}\sum_{m=1}^{N_y} A_{ik}^{(1)} B_{jm}^{(1)} w_{km} = 0 \\ &i = 1, N_x; \quad j = 1, ..., N_y \end{aligned} \tag{26}$$

$$
\begin{aligned}
&y = 0, b; \quad w_{ij} = 0; \\
&D_{12}(x,y) \sum_{k=1}^{N_x} A_{ik}^{(2)} w_{kj} - D_{22}(x,y) \sum_{m=1}^{N_y} B_{jm}^{(2)} w_{im} - 2D_{26}(x,y) \sum_{k=1}^{N_x} \sum_{m=1}^{N_y} A_{ik}^{(1)} B_{jm}^{(1)} w_{km} = 0 \\
&i = 1, ..., N_x; \quad j = 1, N_y
\end{aligned}
\tag{27}
$$

Similarly, the other boundary conditions can be represented using DQM. The domain and boundary equations are assembled to yield to set of linear equations,

$$
\begin{bmatrix} K_{bb} & K_{bd} \\ K_{db} & K_{dd} \end{bmatrix} \begin{Bmatrix} w_b \\ w_d \end{Bmatrix} = N_{vat} \begin{bmatrix} 0 & 0 \\ F_{db} & F_{dd} \end{bmatrix} \begin{Bmatrix} w_b \\ w_d \end{Bmatrix} \tag{28}
$$

where N_{vat} is the buckling load and w is the mode shape. Solving the above Eq. 28 (eigenvalue problem) yields the buckling load and mode shapes of symmetrical vat plate.

6. Results and Discussion

The prebuckling and buckling results of VAT panels subjected to different loading conditions are presented in this section. For the numerical simulation, the material properties for each lamina are chosen as, E_1= $181GPa$, E_2= $10.27GPa$, G_{12}= $7.17GPa$, ν_{12}= 0.28 with thickness t=$1.272\times10^{-4}m$. In order to validate the DQM results, finite element (FE) modelling of the VAT panels was carried out using ABAQUS. The S4 shell element was chosen for discretization of the VAT plate structure and appropriate mesh density was selected to achieve the required accuracy. Each FE element was assumed to have a constant fiber orientation in order to model the linear fibre angle distribution within each of the lamina. The thickness variation of the VAT plate due to tow overlap or gaps were not considered in the present study.

6.1. Prebuckling response of VAT plate subjected to cosine loading

To validate the generality of the stress function based formulation, prebuckling analysis of anisotropic VAT plates subjected to pure stress boundary conditons was studied using DQM and the results were compared with FE analysis results. A square VAT plate (a=b=$1m$) subjected to in-plane compressive cosine distributed load $\sigma_0 cos(\frac{\pi y}{b})$ along the edges $x = 0, a$ and other stress boundary conditons are shown in Fig.1. A symmetric VAT plate

$(0\pm < 45|0 >_{3s})$ was chosen for the in-plane analysis and the number of grid points for DQM modelling was chosen to be N_x=N_y=30. For FE simulation, the mesh density of 40× 40 was selected to analyse the above problem. The stress resultant distributions obtained using DQM and FE results are shown in Fig. 2 and are very close to each other. From Fig. 2, it is seen that $\bar{N}_x, \bar{N}_y, \bar{N}_{xy}$ distributions obtained using DQM satisfy the specified stress boundary conditions accurately and can be extended to any generalised axial loading distributions.

6.2. Prebuckling response of VAT plate subjected to uniform compression

The proposed stress function methodology was then extended to perform inplane analysis of VAT plate subjected to uniform axial compression (mixed boundary conditons). In this case, a square VAT plate $(0\pm < 0|45 >_{3s})$ is loaded by uniform end shortening, $u_{app} = 0.5mm$, along the edges $x = 0, a$. The stress distribution corresponding to the displacement boundary condition was determined using the least square approach. The number of Legendre polynomial terms were chosen to be 7 for accurate determination of non-uniform axial load distribution along the edges. The number of grid points for DQM modelling was chosen to be N_x=N_y=30. The axial stress distribution along the edges $x = 0, a$ obtained using DQM is shown in Fig. 3 and the results matches very well with FE results. The $\bar{N}_x, \bar{N}_y, \bar{N}_{xy}$ distributions obtained using DQM and FEM are shown in Fig. 4 and the results are closer to each other. The results shows the ability of the proposed DQM formulation to handle mixed boundary conditions along the edges of the plate.

6.3. Buckling response of rectangular VAT plate subjected to uniform compression

Buckling results obtained using DQM for VAT plates subjected to uniaxial compression under various plate boundary conditions are presented in this section. The principle behind improvement of buckling performance of the VAT plate is due to redistribution of the applied load from the center of the plate towards the edges by tailoring the stiffness properties. For simply supported boundary conditons, Gurdal *et. al.* (8) has shown that there was significant improvement in buckling performance of VAT panels, when the loading is perpendicular to the fiber variation direction. DQM analysis was carried for VAT plates under simply supported boundary condition with fiber orientation perpendicular to the loading direction $(90\pm < T_0|T_1 >)_{3s}$

and for different plate aspect ratios. The grid point distribution was assumed to be same ($N = N_x = N_y$) in both the directions of the plate and the same grid distribtuion was used to solve both the Eqns. 14 and 28. The non dimensional buckling coefficient(K_x^{cr}) and stiffness (E_{vat})of VAT plates are evaluated by the following relation,

$$K_x^{cr} = \frac{N_{vat} a^2}{E_1 b h^3}; \quad E_{vat} = \frac{a \int_0^b \bar{N}_x(a, y) dy}{b h u_{app}} \tag{29}$$

The VAT plate configuration $(90\pm < 0|75 >)_{3s}$ which had maximum buckling coefficient was chosen for the numerical convergence study of DQM results. Table. 1 shows the (K_x^{cr}) results obtained using DQM and FE method for VAT plates with different aspect ratios (AR) and various grid point distributions ($N = N_x = N_y$). FE results were computed using fine meshes to get accurate results. For square plates, DQM results were close to the FE results and requires few grid points to get accurate results. As the plate aspect ratio increases, DQM requires more grid points to get better results, but less computational effort compared to FE analysis. The buckling mode shape for a square VAT plate $(90\pm < 0|75 >)_{2s}$ obtained using DQM (N=32)and FE analysis are shown in Fig. 5 and are close to each other.

DQM was then applied to solve the buckling problem of VAT plates under clamped boundary conditions. A rectangular VAT plate $(90\pm < T_0|T_1 >)_{2s}$ with aspect ratio of 10 is considered in this study. The buckling load (N_{vat}) and stiffness (E_{vat}) of VAT plate was normalized with respect to critical buckling load (N_{iso}) and stiffness (E_{iso}) of a quasi-isotropic laminate $[45/-45/0/90]_{2s}$ respectively. This provides a better measure because good composite designs often concerns the selection of laminates that perform better than quasi-isotropic laminates. FE analysis of the VAT plates was carried out using ABAQUS with a mesh density of 200×40 and the number of grid points was chosen to be N_x=N_y=30 for DQM modeling. FE analysis required more S4 elements for clamped boundary conditions when compared to simply supported to get converged buckling load results because of the problems associated with satisfaction of zero slope boundary conditons along the edges of the plate. Normalized values of the buckling load versus stiffness for various VAT plate configurations $(90\pm < T_0|T_1 >)_{2s}$ obtained using DQM and FE method are shown in Fig. 6. The results clearly shows the variation in buckling load for different values of T_0, T_1 and the maximum value is achieved for the VAT plate configuration $(90\pm < 0|80 >)_{2s}$. For this VAT configuration,

Table 1: Buckling Coefficient K_x^{cr} results obtained by DQM and FEM for SSSS VAT plates ($90\pm < 0|75 >$) of different aspect ratio (AR) under axial compression

AR	FEM	RR (8)	DQM				
			N=20	N=24	N=28	N=32	N=36
1	3.067 (40x40)	3.14	3.089	3.0385	3.082	3.079	3.077
4	45.33 (80x20)	-	45.073	45.476	45.605	45.635	45.64
10	283.571 (120x20)	-	254.373	272.119	279.211	283.402	284.004

66.4% increase in buckling load when compared to quasi-isotropic laminate was observed. The mode shape shown in Fig. 7 was computed using DQM with grid point distribution (N=30) and matches very well with FE analysis.

Finally, DQM was extended to study the buckling problem of VAT plates (AR=10) with one edge free edge and all the other simply supported as shown in Fig. 8. In this case, the loads has to be redistributed from the free edge ($y = b$) of the plate to the other edge ($y = 0$) of the plate. In order to achieve this distribution, the fiber orientation was allowed to vary linearly from the free edge of the plate to the other edge of the plate. The number of grid points for DQM modeling was chosen to be N_x=N_y=34 and the mesh density was chosen to be 100×20 for FE analysis. Fig. 9 shows the normalized buckling load versus stiffness results of VAT plates $(90\pm < T_0|T_1 >)_{2s}$ computed using DQM and FE analysis. The VAT plate configuration $(90\pm < 10|80 >)_{2s}$ exhibited high buckling load compared to other linear fiber variations and 85.4% increase in buckling load was observed when compared to quasi-isotropic laminate. The mode shape obtained using DQM and FE analysis are shown in Fig. 10 and the results are close to each other.

7. Conclusion

Differential quadrature methodology based on Airy's stress function approach was proposed to solve the in-plane analysis of VAT plates subjected to cosine distributed compressive loads and uniform axial compression. The in-plane analysis results obtained using DQM matches very well with FE results and shows the ability of DQM to handle stress/displacment boundary conditions effectively with less computational effort. Buckling analysis

of rectangular VAT plates with simply supported, clamped and free edge boundary conditions were carried out using DQM. Comparisons are made with FE results and it was observed that DQM yield accurate results with less grid point distributions. It is observed that the DQM results converge rapidly to the FE analysis and provides information about the minimum number of grid points required to obtain accurate results. The study shows that DQM is fast, accurate and requires less computational effort when compared to FE analysis. This study also shows the accuracy and efficiency of the DQM approach in analysing buckling behavior of VAT plates. In future, DQM will be intergated with optimisation algorithms to design VAT panels with nonlinear fiber variations for improved buckling performance.

8. Acknowledgements

References

[1] Biggers, S. B., Srinivasan, S., Compression buckling response of tailored rectangular composite plates, *AIAA Journal*, Vol. 31(3), 1993, pp. 590-6.

[2] Biggers, S. B., Browder, T. M., Buckling load interaction in tailored composite plates, *Composites Engineering*, Vol. 4(7), 1994, pp. 745-61.

[3] Hyer, M. W., Charette, R.F., The use of curvilinear fiber format in composite structure design, *AIAA Journal*, Vol. 29(6), 1991, pp. 1011-5.

[4] Hyer, M.W., Lee, H.H., The use of curvilinear fiber format to improve buckling resistance of composite plates with central circular holes, *Composite Structures*, Vol. 18, 1991, pp. 239-61.

[5] Nagendra, S., Kodilyam, S., Davis, J. E., Optimization of tow fiber paths for composite design, *36th AIAA/ASME/ASCE/AHS/ASC Structures, Structural Dynamics, and Materials Conference*, 1995.

[6] Gurdal, Z., Olmedo, R., In-plane response of laminates with spatially varying fiber orientations: variable stiffness concept, *AIAA Journal*, Vol. 31(4),1993, pp. 751-58.

[7] Senocak, E. Tanriover, H., Analysis of composite plates with variable stiffness using Galerkin Method, *Aeronautical Journal*, Vol. 111, 2007, pp. 247-56.

[8] Gurdal, Z., Tatting, B.F., Wu, C.K., Variable stiffness composite panels: effects of stiffness variation on the in-plane and buckling response, *Composites: Part A*, Vol. 39, 2008, pp. 911-22.

[9] Alhajahmad, A., Mostafa M. A.,Gurdal, Z., Design tailoring for pressure pillowing using tow-placed steered fibers, *Journal of Aircraft*, Vol. 45(2), 2008, pp. 630-40.

[10] Weaver, P. M., Potter, K. D., Hazra, K., Saverymuthapulle, M. A. R., Hawthorne, M. T., Buckling of variable vngle tow plates: from concept to experiment, *50th AIAA/ASME/ASCE/AHS/ASC Structures, Structural Dynamics, and Materials Conference*, 2009.

[11] Bellman, R.E., Casti, J., Differential quadrature and long-term integration, *J Math Anal Appl*, Vol. 34, 1971, pp. 235-38.

[12] Shu, C.,*Differential quadrature and its application in engineering*, London: Springer-Verlag, 2000.

[13] Jang, S. K., Bert, C. W., Striz, A. G., Application of differential quadrature to static analysis of structural components, *Int. J. Numer. Methods in Engg.*, Vol. 28, 561-77, 1989.

[14] Sherbourne, A. N., Pandey M. D., Differential quadrature method in the buckling analysis of beams and composite plates, *Comput Struct*, Vol. 40, 1991, pp. 90313.

[15] Darvizeh, M., Darvizeh, A., Ansari, R., Sharma, C. B., Buckling analysis of generally laminated composite plates (generalized differential quadrature rules versus RayleighRitz method), *Composites and structures*, Vol. 63, 2004, pp. 69-74.

[16] Wang, X., Gan, L., Zhang, Y., Differential quadrature analysis of the buckling of thin rectangular plates with cosine-distributed compressive loads on two opposite sides, *Advances in Engineering Software*, Vol. 39, 2008, pp. 497-504.

[17] Shu, C., Du, H., Implementation of clamped and simply supported boundary conditions in the GDQ free vibration analysis of beams and plates, *Int. J. Solids and Structures*, Vol. 34, 1997, 819-835.

[18] Shu, C., Chen, W., On optimal selection of interior points for applyin discretized boundary conditions in DQ vibration analysis of beams and plates, *J. of Sound and Vibration*, Vol. 222(2), 1999, 239-257.

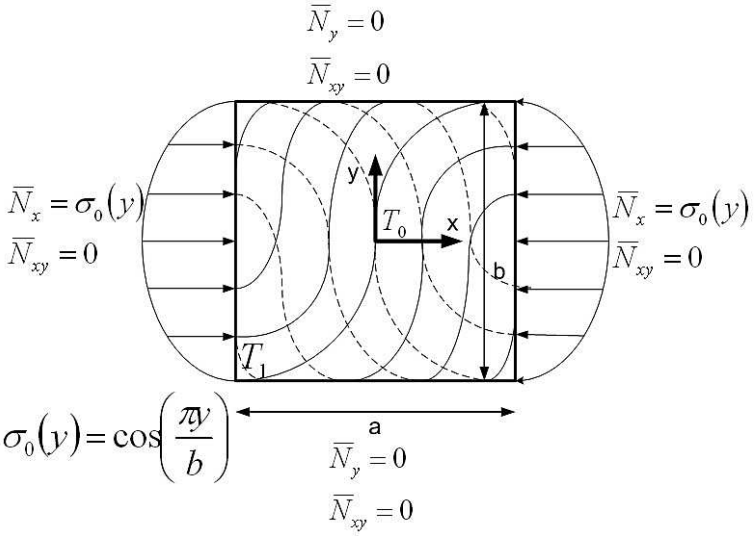

Figure 1: Square VAT plate subjected to cosine distributed edge load.

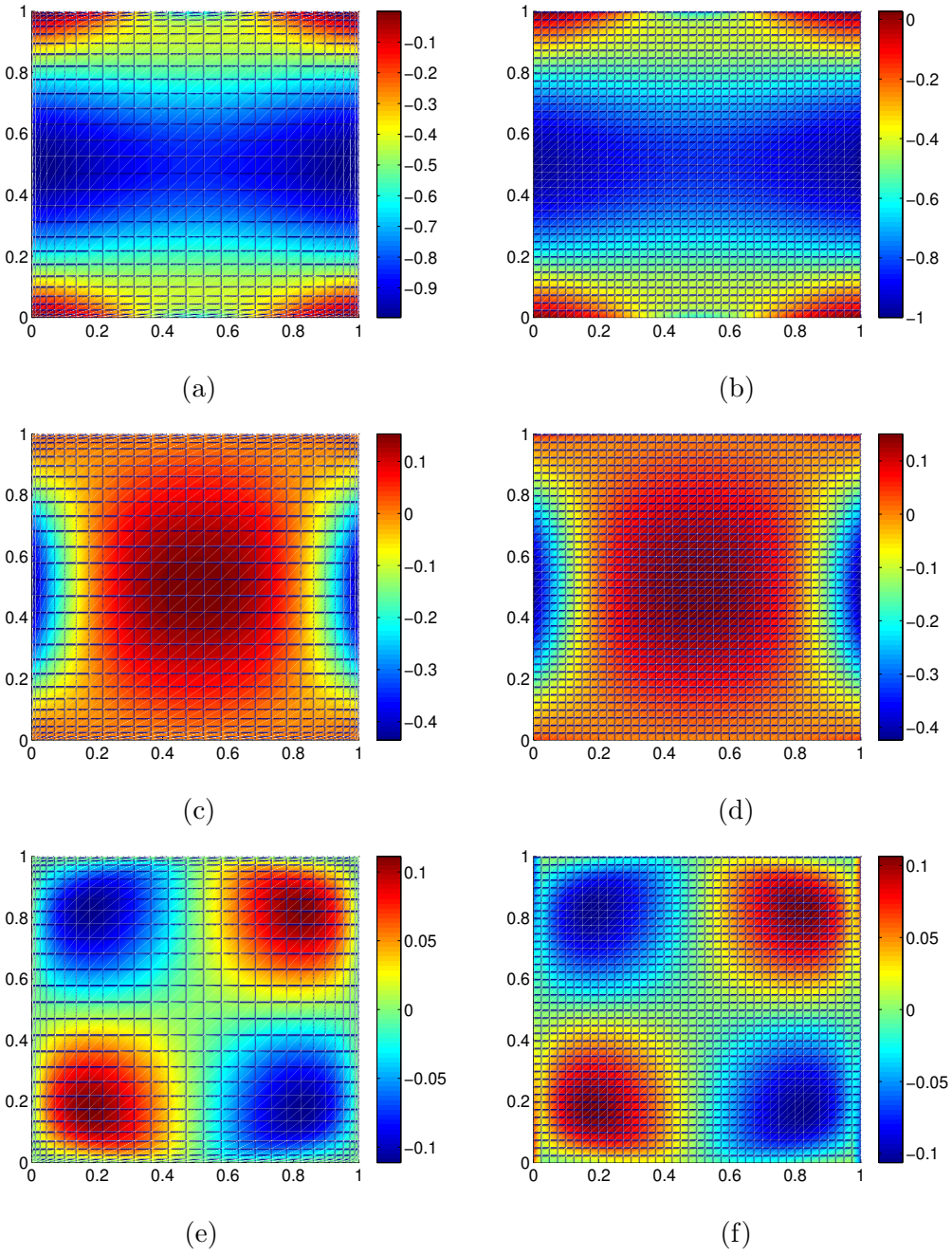

Figure 2: Stress resultant distributions of VAT plate ($0\pm < 45|0 >_{3s}$) subjected to cosine distributed edge load: (a) $\bar{N}_x$ (DQM) (b) $\bar{N}_x$ (FEM) (c) $\bar{N}_y$ (DQM) (d) $\bar{N}_y$ (FEM) (e) $\bar{N}_{xy}$ (DQM) (f) $\bar{N}_{xy}$ (FEM).

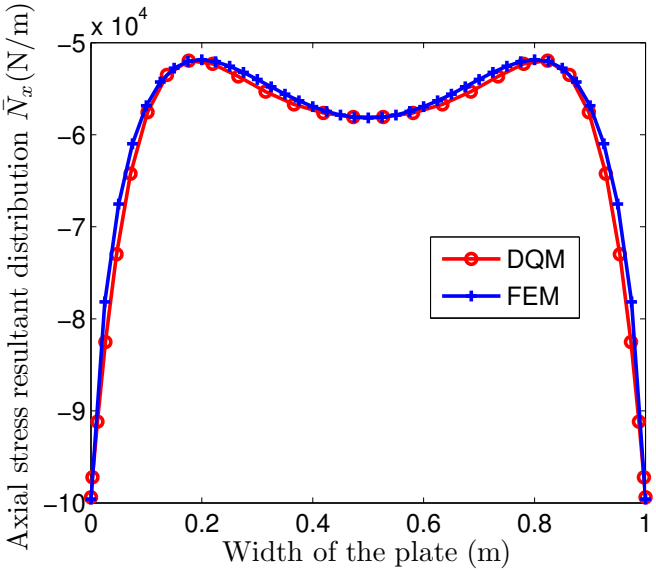

Figure 3: Square VAT plate $(0\pm < 0|45 >_{3s})$ subjected to axial compression: Axial stress resultant distributions along the edge $x = a$ computed using DQM and FEM.

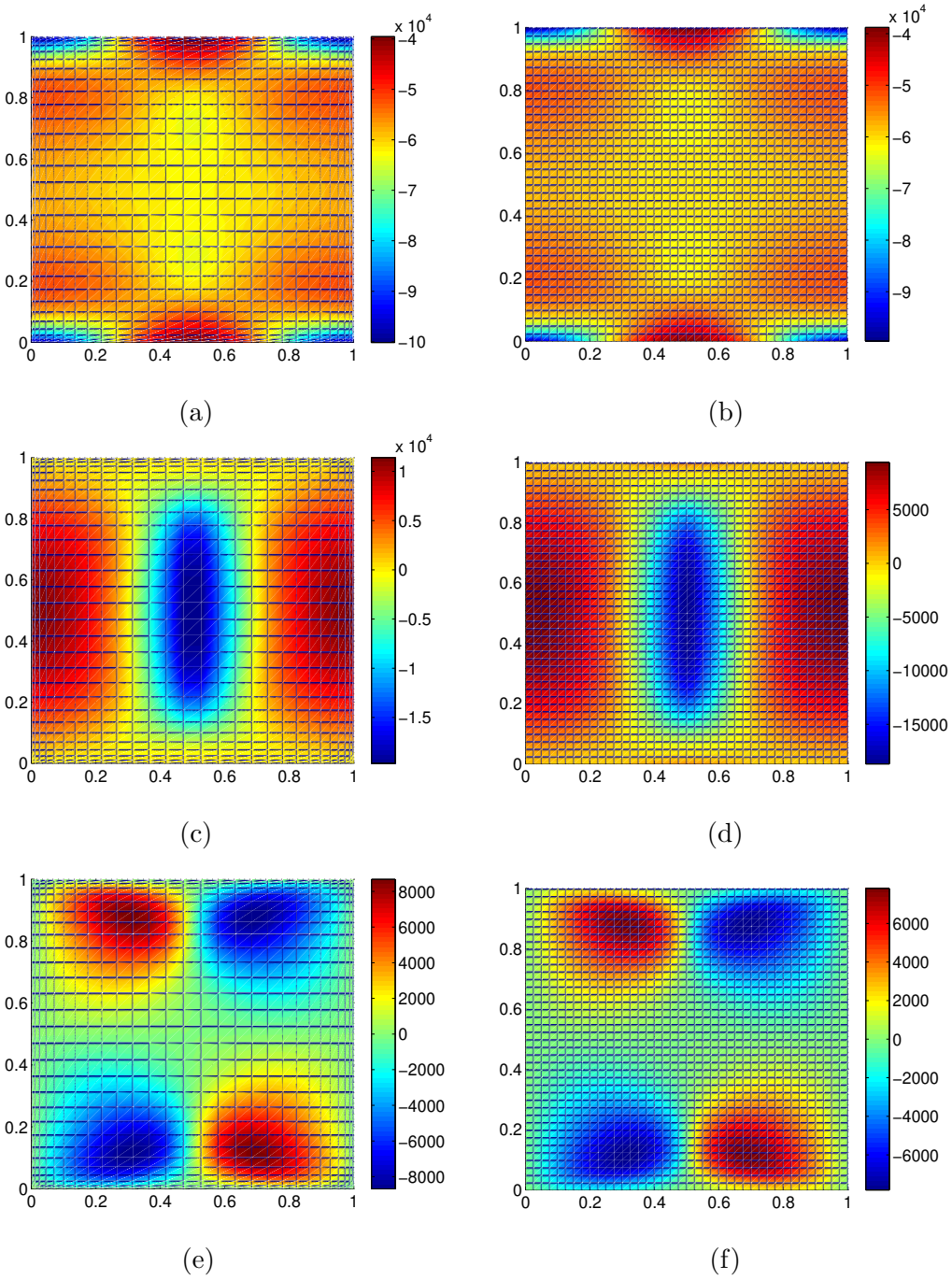

Figure 4: Stress resultant distributions of VAT plate ($0\pm < 0|45 >_{3s}$) subjected to axial compression: (a) $\bar{N}_x$ (DQM) (b) $\bar{N}_x$ (FEM) (c) $\bar{N}_y$ (DQM) (d) $\bar{N}_y$ (FEM) (e) $\bar{N}_{xy}$ (DQM) (f) $\bar{N}_{xy}$ (FEM).

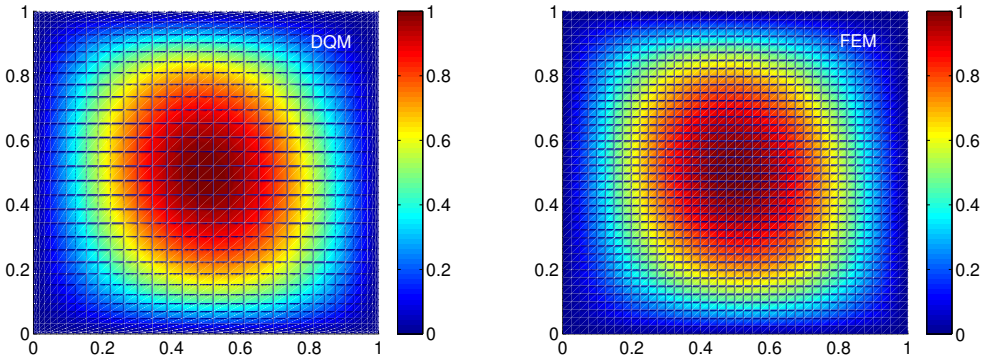

(a) (b)

Figure 5: Buckling mode shape of square VAT plate $(90\pm < 0|75 >)_{2s}$ (a) DQM (b) FEM.

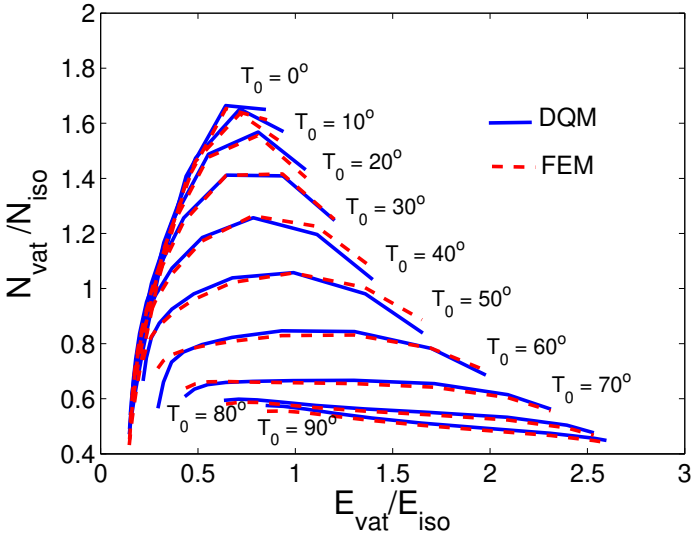

Figure 6: VAT plate $(90\pm < T_0|T_1 >)_{2s}, AR = 10$ subjected to axial compression and clamped boundary conditions : Normalized Buckling load ratio Vs Normalized stiffness variation obtained using DQM and FEM for different T_0, T_1.

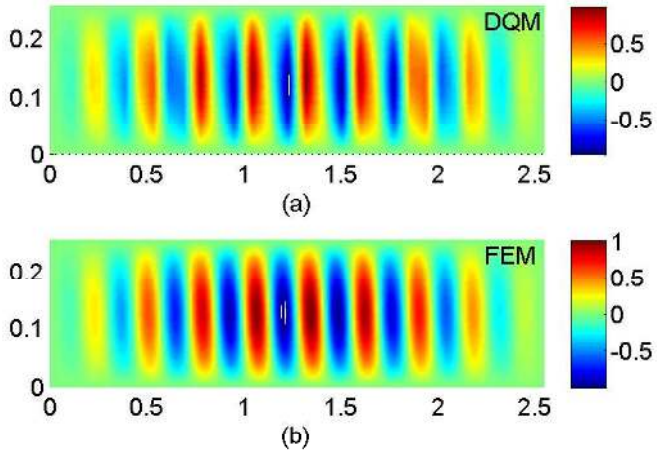

Figure 7: Buckling mode shape of VAT plate $(90\pm < 0|80 >)_{2s}, AR = 10$ with clamped boundary conditions (a) DQM (b) FEM.

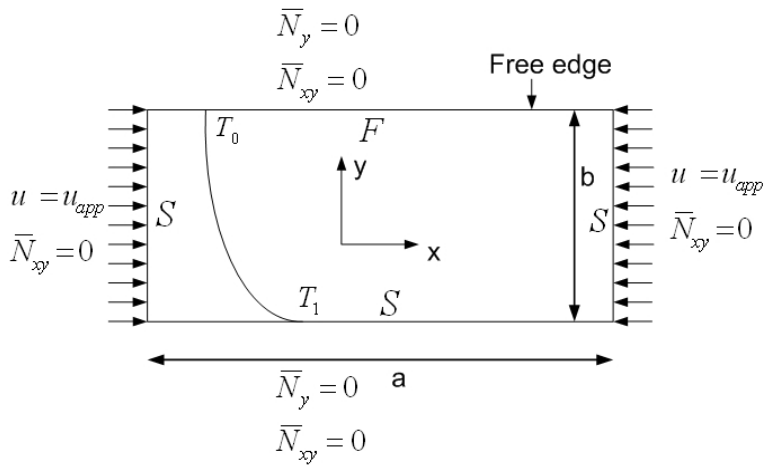

Figure 8: Rectangular VAT panels under axial compression and SSSF boundary condition showing the linear fiber angle variation and applied boundary conditions.

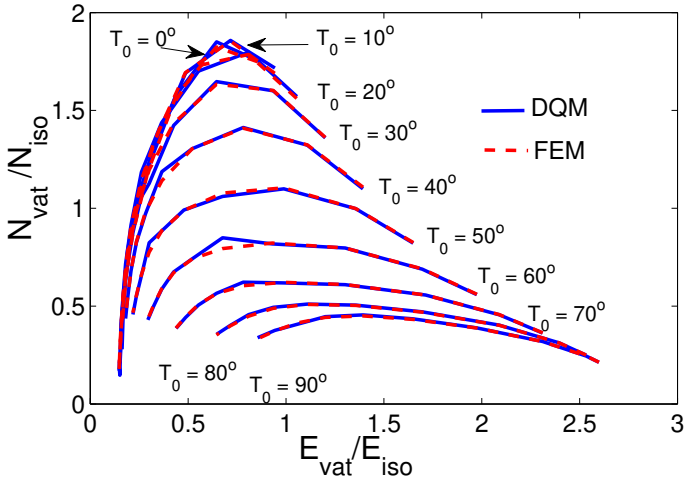

Figure 9: VAT plate $(90\pm < T_0|T_1 >)_{2s}, AR = 10$ subjected to axial compression and SSSF boundary condition : Normalized Buckling load Vs Normalized stiffness variation obtained using DQM and FEM for different T_0, T_1.

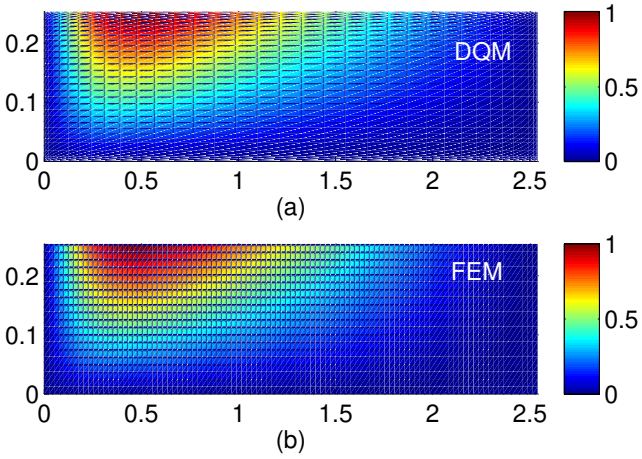

Figure 10: Buckling mode shape of VAT plate $(90\pm < 10|80 >)_{2s}, AR = 10$ with SSSF boundary condition (a) DQM (b) FEM.